Molecular dynamics study of aging effects in supercooled Al$_2$O$_3$

Vo Van Hoang[1,*] and Suhk Kun Oh[2]

[1]*Department of Physics, College of Natural Sciences, HochiMinh City National University, 227 Nguyen Van Cu Str., Distr. 5, HochiMinh City, Vietnam*
[2]*Department of Physics, Chungbuk National University, Cheongju 361-763, South Korea*

Using molecular dynamics simulations we investigated the effect of aging on static and dynamic properties of supercooled Al$_2$O$_3$ models at the temperatures of 2100 K and 5600 K. Simulations were done in the basic cube under periodic boundary conditions containing 3000 ions with Born-Mayer type pair potentials. We obtain the changes as a function of time for the total energy and density of the system. The aging time dependence of partial radial distribution functions (PRDFs), coordination number distributions and bond-angle distributions has been studied. We compare the PRDFs for the 10% most mobile Al or O atoms with the corresponding mean PRDFs. We find the effect of aging on the dynamical heterogeneities in the system. Al and O atoms show similar dynamical heterogeneities but with a differing rate of changes during aging. Furthermore, we also find significant aging effects in mean-squared atomic displacement and diffusion constant.

I. INTRODUCTION

Aging effects in supercooled glasses have been under intensive investigation for a long time. Miyagawa and Hiwatari carried out molecular dynamics simulations on a soft-sphere model for binary alloys quenched into glassy states at different rates [1]. The main purpose of their work was to investigate slow relaxation phenomena of the quenched glassy states close to the glass transition by calculating both the static and dynamical structural changes upon aging (annealing) of them. It was shown that the static properties exhibit neither significant change during annealing of samples, nor changes for different samples. However, the dynamic properties show remarkable aging effects as well as sample-dependent behavior, meaning that the quenched glassy state cannot attain an equilibrium state for the time scale of simulations, due to dynamical slowing-down phenomena [1]. The quenched sample was shown to tend to a seemingly quasi-equilibrium state after a sufficient annealing. Detailed discussions on both aging effects and sample-dependent behaviors of quenched glassy states was made, by paying attention to the behavior of the single-atom motion, mean-squared displacement, and self-diffusion constant of the quenched glassy states [1]. The effects of aging and drying on the structure of V$_2$O$_5$ gels have been obtained experimentally [2]. Semiconducting V$_2$O$_5$ gels with and without addition of GeO$_2$ were prepared by hydrolysis of metal alkoxides in alcoholic solutions. They found that crystalline vanadium oxides were not observed in xerogels, but V$_3$O$_7$ diffraction peak was found for the aerogels kept at 250 °C and 210 atm for 2 h or longer before drying. However, the aging effects can be studied in more details only by the computer simulation, and historically, computer simulations have perhaps had their largest impact on the fundamentals of materials science in the study of amorphous systems. We can find numerous simulation works concerning on the aging effects in different systems.

Using molecular dynamics simulations, Kob *et al.* studied the out of equilibrium dynamic correlations in a model glass-forming liquid [3]. The system was quenched from a high temperature to a temperature below its glass transition temperature, and the decay of the two-time intermediate scattering function $C(t_w, t+t_w)$ was monitored for several values of the waiting time t_w after the quench. They found that $C(t_w, t+t_w)$ showed a strong dependence on the waiting time, i.e., aging, depended on the temperature before the quench, and similar to the case of spin glasses, it could be scaled onto a master curve. In Ref. [4], Poliwa and Heuer presented simulations of a hard disk system and analyzed the time evolution of the dynamical heterogeneities, and they characterized the time evolution of slow regions and slow particles individually. Also, using molecular dynamics simulations Kerrache *et al.* [5] investigated the presence of dynamical heterogeneities in supercooled silica, a strong glass former. They also studied the changes as a function of time for these dynamical heterogeneities during aging. They compared the radial distribution function for the 10% most mobile Si or O atoms with the corresponding mean radial distribution functions. They also measured changes in these radial distribution functions and the changes in the non-Gaussian parameter with time after a quench, and they found that dynamical heterogeneities increased during the aging process. Recently, the cooling rate, heating rate, and aging effects in glassy water have been comprehensively investigated [6]. In this work, the authors reported a molecular dynamics simulation of the properties of the potential energy landscape sampled by a system of water molecules during the process of generating a glass by cooling, and during the process of regenerating the equilibrium liquid by heating the glass. They have studied the dependence of these processes on the cooling/heating rates as well as on the role of aging (the time elapsed in the glass state). However, the aging effects in the supercooled Al$_2$O$_3$ have not been investigated yet. And therefore,

_____

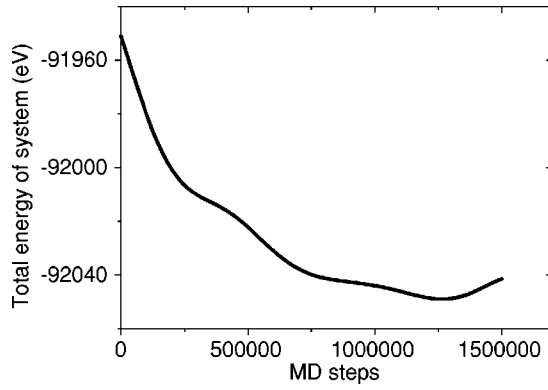*Email address: vvhoang2002@yahoo.com

FIG. 1. Aging time dependence of total energy in the Al_2O_3 system.

this problem has been studied in details by investigating the dependence of static and dynamic properties of supercooled Al_2O_3 on aging.

II. CALCULATION

We perform MD simulations of Al_2O_3 models containing 3000 ions. The Born-Mayer type pair potential used here is of the form

$$u_{ij}(r) = z_i z_j \frac{e^2}{r} + B_{ij} \exp\left(-\frac{r}{R_{ij}}\right), \qquad (1)$$

where the terms represent Coulomb and repulsion energies, respectively. Here r denotes the distance between the centers of ith and jth ions; z_i and z_j are the charges of ith and jth ions; B_{ij} and R_{ij} are the parameters accounting for the repulsion of the ionic shells. Values $z_1 = +3$ and $z_2 = -2$ are the charges of Al^{3+} and O^{2-}. The values $B_{11} = 0$, $B_{12} = 1779.86$ eV, $B_{22} = 1500$ eV and $R_{ij} = 29$ pm were corrected from the potential used in [7] to obtain a good agreement with experiment for atomization energy and for the partial radial distribution functions (PRDFs) of models, and these parameters are close to the ones used in [7]. Coulomb interaction was taken into account by the Ewald-Hansen method [7–12]. System was cooled down from equilibrium liquid
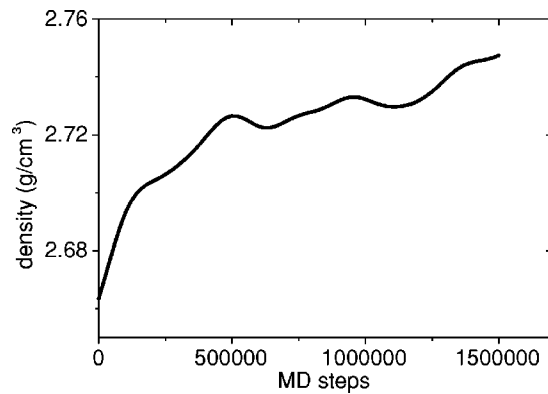

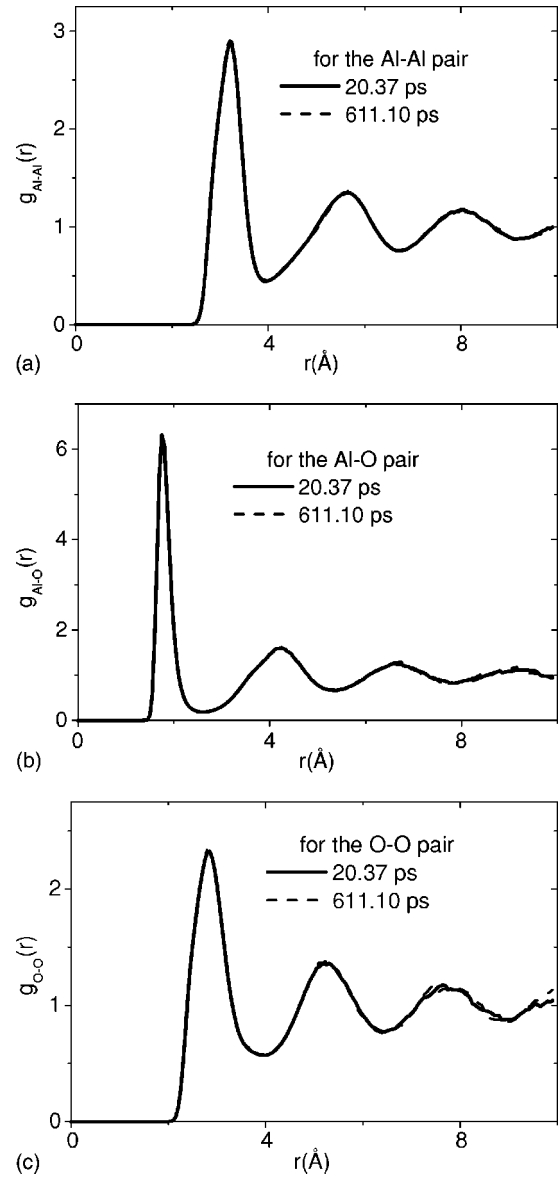FIG. 2. Aging time dependence of the density in the Al_2O_3 system.

FIG. 3. Radial distribution function in the supercooled Al_2O_3 models obtained after different aging times of 20.37 ps and 611.10 ps.

model at 7000 K with cooling rate 1.7178×10^{14} K/s and at constant pressure $P = 0$ GPa. Using the Born-Mayer potential (1) we have successfully simulated structure and properties of liquid and amorphous Al_2O_3 [13–16]. Our simulations were done at constant pressure ($P = 0$). We use the Verlet algorithm [13] with the MD time step 4.0749×10^{-16} s. We study the system at the temperatures of 5600 K and 2100 K. At each temperature, the system was equilibrated for 50 000 or 1 500 000 MD time steps before evaluating the quantities. It is essential to notice that the typical time of equilibration of the Al_2O_3 system was considered about 10 000 MD time steps [13]. The density of the model at the temperature of 2100 K is equal to 2.70 g/cm^3 and is close to the experimental data [17], e.g., 2.81 g/cm^3. Calculated energy of supercooled Al_2O_3 model at the temperature of 2100 K is equal to 14 745 kJ mol^{-1} and is close to that of real crystal Al_2O_3,

TABLE I. Structural characteristics of supercooled Al_2O_3 at the temperature of 2100 K. r_{ij}: Positions of the first peaks in the partial radial distribution functions (PRDFs) $g_{ij}(r)$; g_{ij}: The heights of the first peaks in PRDFs; Z_{ij}: The average coordination number(1-1 for the Al-Al pair, 1-2 for the Al-O pair, 2-1 for the O-Al pair, and 2-2 for the O-O pair). (∗) Experimental data at the temperature of 2473 K in [17,20].

Aging time (ps)	r_{ij} (Å)			g_{ij}			Z_{ij}			
	1-1	1-2	2-2	1-1	1-2	2-2	1-1	1-2	2-1	2-2
20.37	3.21	1.76	2.83	2.88	6.36	2.33	7.85	4.22	2.81	8.19
407.4	3.21	1.77	2.81	2.93	6.28	2.37	7.98	4.23	2.82	8.40
611.1	3.21	1.77	2.81	2.90	6.27	2.35	8.03	4.23	2.82	8.38
∗	3.25	1.78	2.84	1.70	5.60	2.40		4.20		

which is about 15 300 kJ mol^{-1} [7]. Therefore, the Born-Mayer potential with such effective charges for Al cation and O anion exhibits the real atomization energy of supercooled Al_2O_3 well. Equilibrium configurations obtained from MD simulations are employed to calculate structure and properties. The pressure in the model is calculated in two terms through Coulomb interaction and short range interaction [18]. For the short range interaction we use the virial formula [18,19] and all calculations in this work were carried out under constant pressure ($P=0$ GPa). Zero pressure is established using the size correction of the basic cube. We may simulate the model at different cube sizes and find the true size by interpolating to zero pressure. Indeed, the pressure fluctuates in the MD run but we can establish the mean pressure to be almost equal to zero. In order to calculate coordination number distributions and bond-angle distributions in the supercooled Al_2O_3 we adopt the fixed values R_{Al-Al} =3.7 Å, R_{Al-O}=2.2 Å, and R_{O-O}=3.3 Å, where R denotes a cutoff radius, which is chosen as the position of the minimum after the first peak in the radial distribution function $g_{ij}(r)$ for the amorphous state at the zero temperature.

III. RESULTS AND DISCUSSIONS

A. Evolution of total energy and density of the system upon aging

Figure 1 shows the evolution of total energy of the system in aging process, the time on abscissa begins with the final MD step of the quenched supercooled sample at the temperature of 2100 K. It is clearly seen that the behavior of the total energy in an early time window such as $0 \leqslant n \leqslant 500,000$ (n denotes the MD time steps number), which we call time region I, differs from that at the later time window of $500\,000 \leqslant n \leqslant 1\,500\,000$ (e.g., time region II). Total energy

TABLE II. Coordination number distribution for the pair Z_{Al-O} in supercooled state after different aging times.

Z_{Al-O}	2	3	4	5	6
Number of Al^{3+} ions (after 20.37 ps)	1	71	729	331	5
Number of Al^{3+} ions (after 407.4 ps)	0	61	811	315	13
Number of Al^{3+} ions (after 611.1 ps)	1	57	816	312	14

in the former time region is high and decreases with increasing time, indicating the sample to be far from an equilibrium state, while in the later time region it fluctuates around a steady value so as to be regarded as a quasi-equilibrium state. Such a phenomenon had been obtained for the binary soft-sphere glasses [1], or for Lennard-Jones glass [3]. However, the difference between the maximum and minimum total energies is very small, i.e., is less than 0.1%. Another quantity of the system we would like to study is the density. We can see in Fig. 2 that the aging time dependence of density of the system also has two time regions like that for total energy. In the region I, the density of the system strongly increases and reaches the steady value anywhere around of 2.74 g/cm^3 in the time region II (see Fig. 2). It is essential to notice that the experimental value for the density of liquid Al_2O_3, at the temperature of 2473 K is about 2.81 g/cm^3 [17] and the density of the system in the equilibrium state close to this one is measured in practice.

B. Effect of aging on static properties

It was stated that the static properties of glasses do not significantly depend on the aging [1]. However, the study was carried out only for the simple model glasses such as soft-sphere glasses or Lennard-Jones systems [1,3] and in more realistic models of glasses it may be different from that ones. Therefore, the systematic investigation of the aging
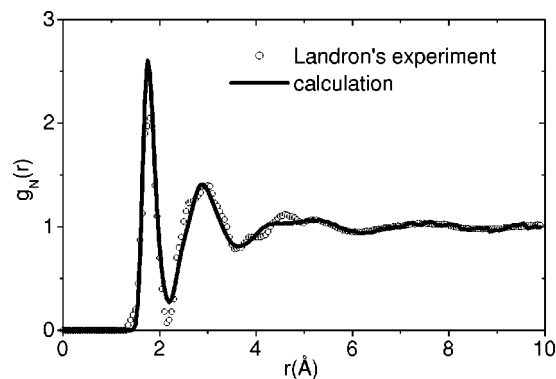

FIG. 4. Total neutron radial distribution function $g_N(r)$ of supercooled liquid Al_2O_3 model at the temperature of 2100 K and experimental data of liquid Al_2O_3 at 2473 K in [17].
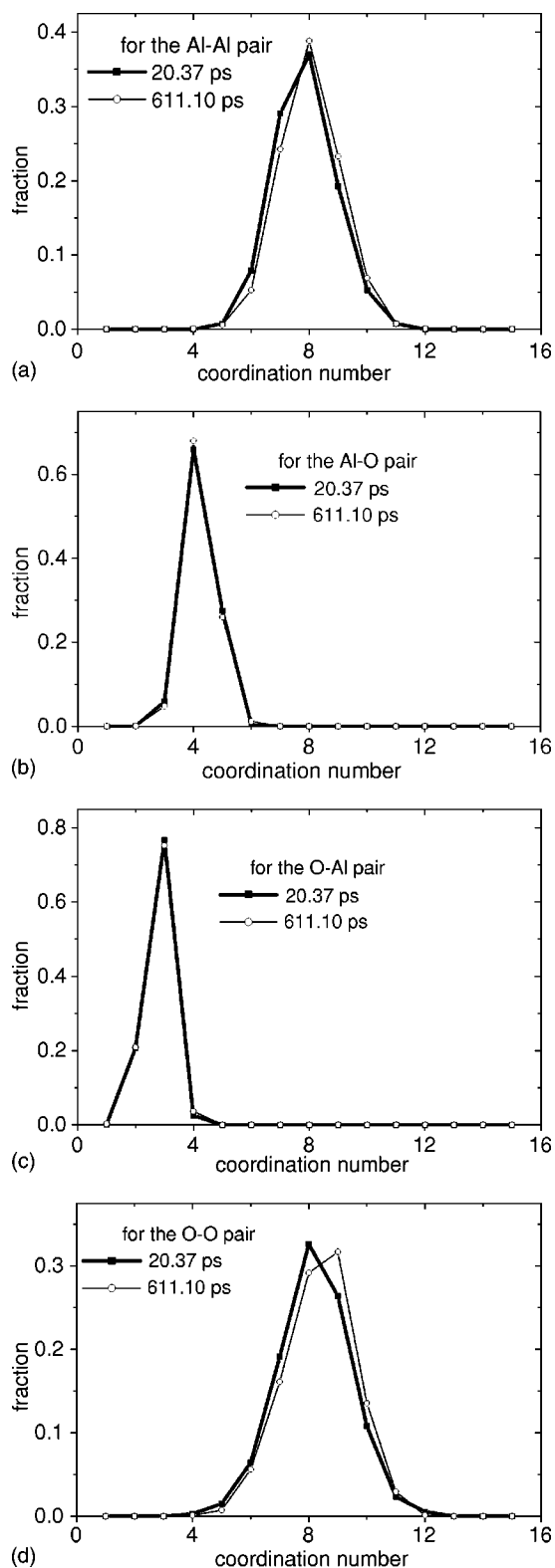
FIG. 5. Coordination number distributions in supercooled Al_2O_3 model at the temperature of 2100 K obtained after two different aging times.

effects on static properties of supercooled Al_2O_3 model at the temperature of 2100 K was done in this work.

First quantity we would like to discuss is the partial radial distribution function (PRDF). As presented in Fig. 3, no ag-

ing effect on PRDF was found. It seems that it is very difficult to detect the effect of aging on average quantities such as PRDF. On the other hand, the structure of our supercooled Al_2O_3 model is in good agreement with experimental data in [17,20]. All structural characteristics in supercooled model slightly change with aging (see Table I). The average coordination number for all pair of atoms slightly increases with aging related to more dense packing structure upon aging, and is in good accordance with increasing density in the system (see Fig. 2). As presented in [17,20] liquid Al_2O_3 has the structure of a tetrahedral network with the average coordination number $Z_{Al-O} \sim 4$. The structural element of network is a slightly distorted $(AlO_4)^{5-}$ tetrahedron. The same structure also exists in our models (see Table I).

We can see network structure of supercooled Al_2O_3 through the coordination number distribution of Al^{3+} ions for the Al-O pair after different aging times (Table II). As shown in Table II, Al atoms are mainly surrounded by four oxygen atoms and the fraction of Al atoms having fourfold coordination increases with aging. In contrast, the number of Al atoms having fivefold coordination decreases. Fraction of Al atoms having other coordination is very small (e.g., threefold or sixfold). Combining this information with the interatomic distances, we may confirm that the elementary unit of the Al_2O_3 system consists of a distorted $(AlO_4)^{5-}$ tetrahedron. The other basic unit is fivefold coordinated polyhedron AlO_5 with significant amount. This means that we find more or less random mixing of fourfold and fivefold configurations in the structure of supercooled Al_2O_3 models and it is in good agreement with recent experimental data for liquid alumina [21].

We also calculate the total radial distribution function for neutron scattering $g_N(r)$ [details about calculation of $g_N(r)$ can be seen in [13]] and it agrees well with experiment data in [17] (see Fig. 4). Now, we turn our attentions to the effect of aging on the microstructure of the system. Figures 5 and 6 show slight changes in coordination number distributions and in bond-angle distributions in the systems obtained after two different aging times of 20.37 ps (or equivalent 50 000 MD time steps) and of 611.10 ps (or equivalent 1 500 000 MD time steps).

Figure 5(a) shows that most of the Al atoms are surrounded by 8 Al atoms in good accordance with the calculated data in Ref. [22], and coordination number distribution for the Al-Al pair significantly depends on aging. The aging leads to increase in the coordination number for the Al-Al pair or to more dense packing between corner-sharing tetrahedral units AlO_4. In contrast, the coordination number distribution for the Al-O pair almost does not change with aging, and most of Al atoms are surrounded by 4 oxygen atoms [see Fig. 5(b)]. This means that tetrahedral network structure of the system does not depend on aging. The same phenomenon for the O-Al pair is also observed as in Fig. 5(c). Although most of oxygen atoms are surrounded by 6 oxygen atoms, the coordination number distribution for the O-O pair also significantly depends on aging [see Fig. 5(d)] and it is related to more dense packing structure of the system upon aging.

Further information about local structural units is provided by the bond-angle distribution. In Fig. 6, we display
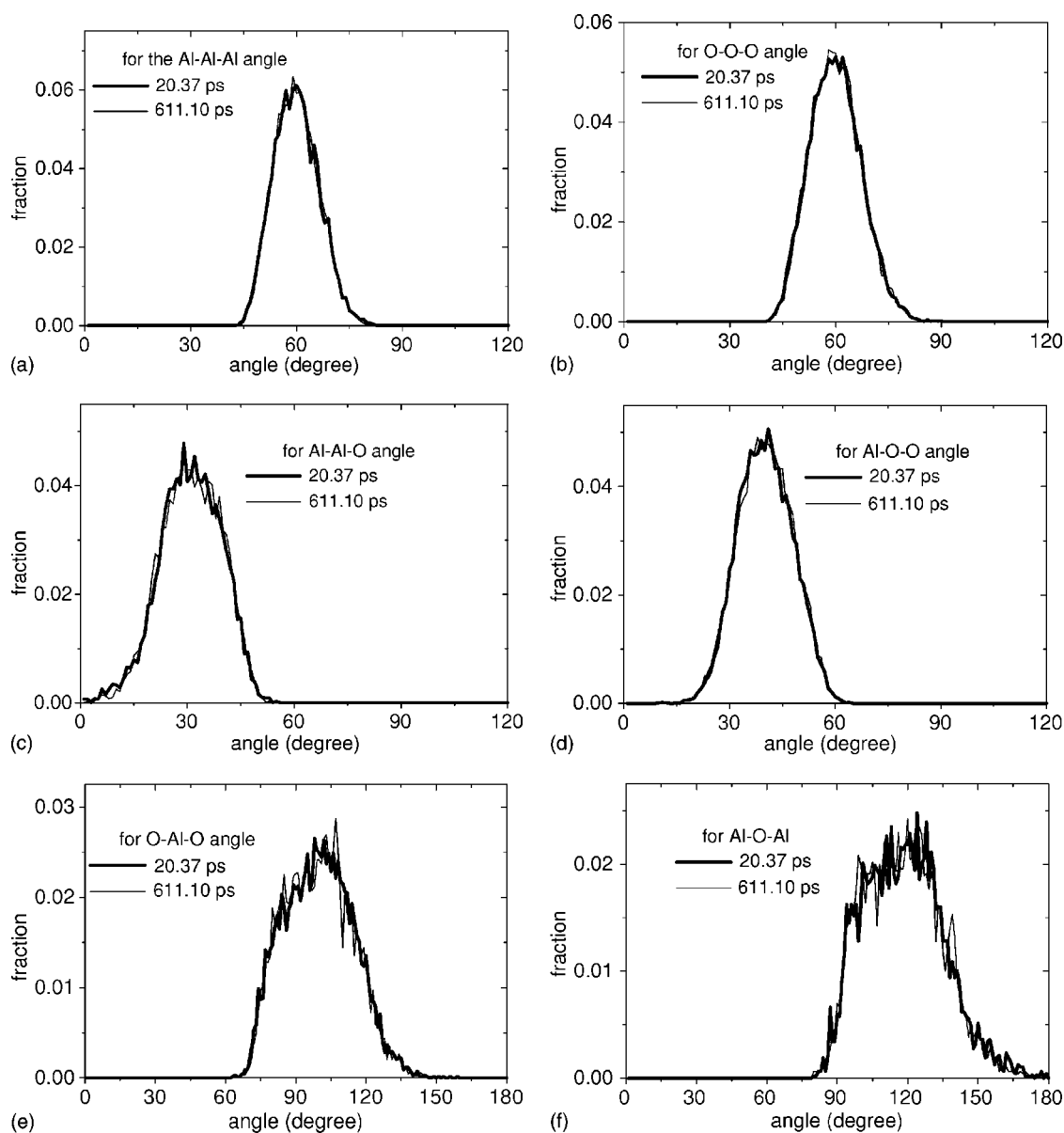
FIG. 6. Bond-angle distributions in supercooled Al_2O_3 model at the temperature of 2100 K obtained after two different aging times.

the bond-angle distribution calculated with Al-Al, Al-O and O-O cutoff distances of 3.7, 2.2 and 3.3 Å, respectively. From the coordination number distributions, we infer that the basic unit is a tetrahedral AlO_4 and such network structure almost does not depend on aging. We can get more details inside the aging dependence of local structure of the system through the bond-angle distributions. It is well known that for an ideal tetrahedron the O-Al-O bond angle is equal to 109.47°, the O-O-O angle is 60°, and the Al-O-O angle is 35.26°. The deviations from these values would indicate the amount of distortion with respect to an ideal tetrahedron. All bond-angle distributions can be seen in Fig. 6, and we can see that such distributions slightly change with aging. The Al-Al-Al bond-angle distribution has a peak at around 60°, O-O-O has a peak at 60°, Al-O-O has a peak at 37°, Al-Al-—O has a main peak 29°, O-Al-O has a main peak at 107°, and Al-O-Al presents main peak at around 120°–

125°. Such bond-angle information confirms our conclusion above that the elementary unit of the system mainly consist of a slightly distorted $(AlO_4)^{5-}$ tetrahedron.

C. Effect of aging on dynamic properties

The dynamic properties of glassy states are currently of great interest, because recent theoretical developments, based on the mode-coupling theory, have pointed out the dynamical origin of the glass transition [1,4,5]. And dynamical heterogeneities in supercooled glasses are the focus of recent investigations [5,23–25]. So far, the effect of aging on the dynamic properties, in particular, on dynamical heterogeneities is not so much investigated (see in [5]). To detect the presence of dynamical heterogeneities people investigated the time dependence of the self-part $G_s(r,t)$ of the van Hove correlation function [26]. For homogeneous system, $G_s(r,t)$
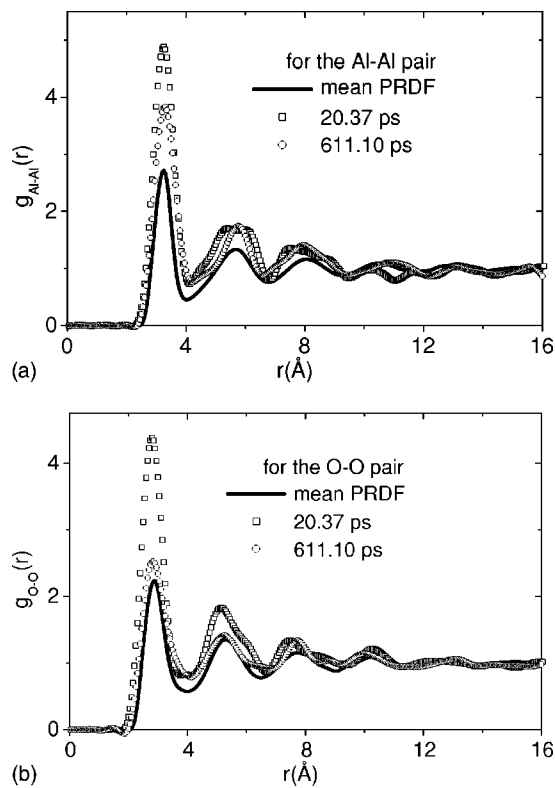
FIG. 7. Partial radial distribution function between the mean Al or O atoms (line) and the 10% most mobile Al or O atoms (scatter) in model samples at the temperature of 2100 K obtained after two different aging times of 20.37 ps and 611.10 ps.
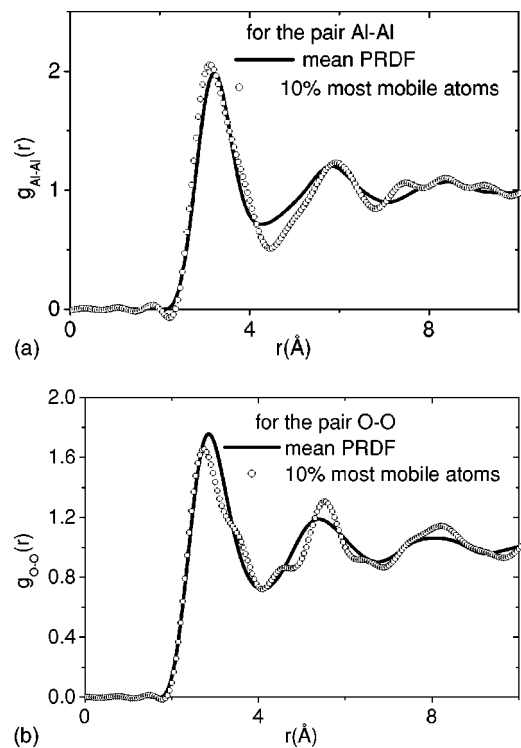

FIG. 8. Partial radial distribution function between the mean Al or O atoms (line) and 10% most mobile Al or O atoms (circles) in the Al_2O_3 models at the temperature of 5600 K.

has a Gaussian form and deviations from this form in simulations of glass-forming liquids are due to dynamical heterogeneities [5,26,27]. Such deviations can be characterized by non-Gaussian parameter $\alpha_2(t) = 3\langle r^4(t)\rangle/5\langle r^2(t)\rangle^2 - 1$ (see in Ref. [5]), where $\langle r^2 \rangle$ is the mean-squared atomic displacement and $\langle r^4 \rangle$ is the mean-quartic atomic displacement. On the other hand, we can also detect dynamical heterogeneities of the system by comparing of PRDF for the 10% most mobile atoms, with the corresponding mean radial distribution functions. The deviation of PRDF for 10% most mobile atoms from the mean ones can be considered as an evidence of dynamical heterogeneities [5]. Also, the deviation of atomic displacement distribution (ADD) from Gaussian form (or equivalently Brownian motion) is another indication of dynamical heterogeneities that has been recognized in recent MD simulations of glass-forming liquid upon cooling [28]. In this work, we will detect the dynamical heterogeneities in the system through the deviation of PRDF for the 10% most mobile atoms from the mean ones in the supercooled Al_2O_3 models at the temperature of 2100 K, which were thermalized through 50 000 MD steps and 1 500 000 MD steps after quench [29].

As shown in the Fig. 7, the aging effects are observed for all components in the system. Aging reduces dynamical heterogeneities of Al and O atoms. Whereas, the aging enhanced dynamical heterogeneities of Si atoms and no aging was observed for O atoms in supercooled SiO_2 models at the temperature of 3500 K (see in [5]). Such temperature is

much higher than the melting point for SiO_2 system, which is equal to 1983 K (see in [30]) and perhaps it is a specific phenomenon for the dynamical heterogeneities in the silica system. However, potentials used in [5] and in our work are quite different, and as mentioned in [31], dynamical properties of the system more sensitively depend on the potential. It is essential to notice that the melting temperature for Al_2O_3 is equal to 2327 K (see in [22]). This means that our Al_2O_3 system at the temperature of 2100 K is being in the supercooled state.

The PRDF for the 10% most mobile Al or O atoms (circles) compared with the mean PRDF (line) at the high temperature of 5600 K can be seen in Fig. 8. At high temperatures, Al_2O_3 system is dynamically homogeneous and no dynamical heterogeneities are found (see Fig. 8). The dynamical heterogeneities appear during the cooling procedure, and such phenomenon can be observed in the Al_2O_3 models at the lower temperature of 2100 K (see Fig. 7).

In Ref. [1], significant effect of aging on the mean-square displacement and self-diffusion constant of the quenched glassy state of binary soft-sphere system was found. As presented in [1], aging strongly reduced the diffusion constant of atoms. However, such phenomenon has not been investigated yet for a more realistic system. And we can detect it in our suppercooled Al_2O_3. We calculate the mean-square displacement and the corresponding self-diffusion constant of Al and O atoms in two model samples at the temperature of 2100 K, which are obtained after two different aging times. Indeed, the aging strongly reduces both quantities (see Fig. 9). Corresponding self-diffusion constants are, $D^1_{Al} = (4.058 \pm 0.049) \times 10^{-7}$ cm^2/s and $D^1_O = (5.830 \pm 0.069)$
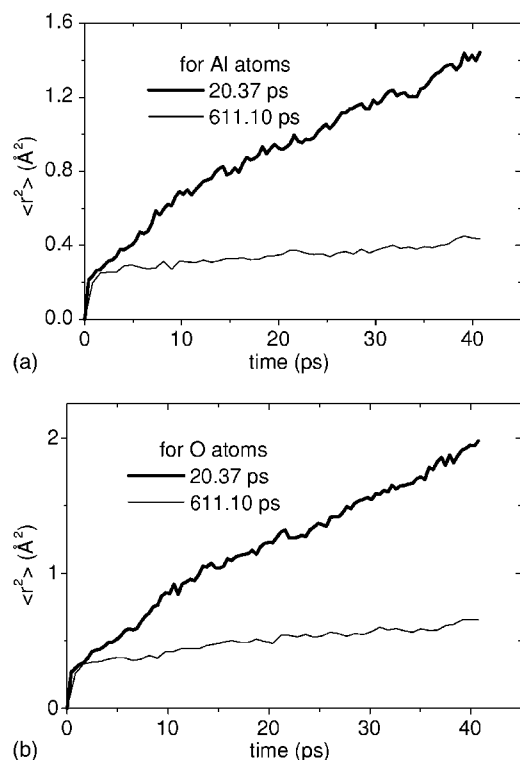
FIG. 9. Mean square displacement of Al or O atoms in model samples at the temperature of 2100 K obtained after two different aging times of 20.37 ps and 611.10 ps.

$\times 10^{-7}$ cm^2/s for the sample obtained after 20.37 ps, $D^2_{Al}=(6.658\pm0.380)\times10^{-8}$ cm^2/s and $D^2_O=(1.155\pm0.054)\times10^{-7}$ cm^2/s for the sample obtained after 611.10 ps, respectively. We have the ratios $D^1_{Al}/D^2_{Al}=6.095$ and $D^1_O/D^2_O=5.048$. It means that the aging strongly reduces the self-diffusion constant of components in the system.

IV. CONCLUSION

In this paper we have investigated the aging effects on both static and dynamic properties of supercooled Al$_2$O$_3$ model at the temperature of 2100 K. Our main conclusions are the following.

(i) Rapidly quenched samples (glasses) are far from equilibrium for relatively long initial times, typically for an order of 500 000 MD time steps upon aging of them. For later times, the system appears to be in a quasiequilibrium state. The density of Al$_2$O$_3$ supercooled system increases with the aging and reaches a steady value after appropriate aging time. This means that aging leads to more dense packing structure of the system.

(ii) Static properties of Al$_2$O$_3$ supercooled system exhibit slight changes upon aging. The aging can cause only small local rearrangement of atoms rather than global changes in the structure (e.g., only small changes in coordination number distributions for the Al-Al and O-O pairs).

(iii) The dynamic properties of Al$_2$O$_3$ supercooled system show remarkable aging effects. Aging reduces dynamical heterogeneities for both Al and O atoms in the system. Furthermore, aging strongly reduces mean square atomic displacement and self-diffusion constant for all components.

[1] H. Miyagawa and Y. Hiwatari, Phys. Rev. A **40**, 6007 (1989).

[2] H. Hirashima, M. Gengyo, C. Kojima, and H. Imai, J. Non-Cryst. Solids **186**, 54 (1995).

[3] W. Kob and Jean-Louis Barrat, Phys. Rev. Lett. **78**, 4581 (1997).

[4] B. Doliwa and A. Heuer, J. Non-Cryst. Solids **307–310**, 32 (2002).

[5] A. Kerrache, V. Teboul, D. Guichaoua, and A. Monteil, J. Non-Cryst. Solids **322**, 41 (2003).

[6] N. Giovambattista, H. E. Stanley, and F. Sciortino, Phys. Rev. E **69**, 050201(R) (2004).

[7] D. K. Belashchenko, Russ. Chem. Rev. **66**, 733 (1997).

[8] M. J. L. Sangster and M. Dixon, Adv. Phys. **25**, 247 (1976).

[9] L. V. Woodcock and K. Singer, Trans. Faraday Soc. **67**, 12 (1971).

[10] D. J. Adams and I. R. McDonald, J. Phys. C **7**, 2761 (1974).

[11] F. Lantelme, P. Turq, B. Quentrec, and J. W. Lewis, Mol. Phys. **28**, 1537 (1974).

[12] J. P. Hansen, Phys. Rev. A **3**, 3096 (1973).

[13] Vo Van Hoang, Phys. Rev. B **70**, 134204 (2004).

[14] Vo Van Hoang and Suhk Kun Oh, Physica B **352**, 73 (2004).

[15] Vo Van Hoang and To Ba Van, The 9th Asia Pacific Physics Conference, Hanoi, 2004.

[16] Vo Van Hoang and Suhk Kun Oh (unpublished).

[17] C. Landron, A. K. Soper, T. E. Jenkins, G. N. Greaves, L. Hennet, and J. P. Countures, J. Non-Cryst. Solids **293–295**, 453 (2001).

[18] Vo Van Hoang and Suhk Kun Oh, J. Phys. B (to be published).

[19] V. V. Wood, *Physics of Simple Liquids Part 2*, edited by H. N. V. Temperly, J. S. Rowlinson, and G. S. Rushbrooke (North-Holland, Amsterdam, 1968).

[20] C. Landron, L. Hennet, T. E. Jenkins, G. N. Greaves, J. P. Coutures, and A. K. Soper, Phys. Rev. Lett. **86**, 4839 (2001).

[21] G. N. Greaves, T. Jenkins, A. Soper, C. Landron, L. Hennet, and J. P. Coutures, available at http://www.estec.esa.nl/conferences/00a06/abstracts/223.html.

[22] G. Gutierrez, A. B. Belonoshko, R. Ahuja, and B. Johansson, Phys. Rev. E **61**, 2723 (2000).

[23] S. C. Glotzer, J. Non-Cryst. Solids **274**, 342 (2000).

[24] D. Bedrov, G. Smith, and J. F. Douglas, Polymer **45**, 3961 (2004).

[25] P. H. Poole, Curr. Opin. Solid State Mater. Sci. **3**, 391 (1998).

[26] J. P. Hansen and I. R. McDonald, *Theory of Simple Liquids* (Academic, London, 1986).

[27] B. Doliwa and A. Heuer, J. Phys.: Condens. Matter **11**, A277 (1999).

[28] G. D. Smith, W. Paul, M. Monkenbush, and D. Richter, J. Chem. Phys. **114**, 4285 (2001).

[29] Because of very slow diffusion in sample after aging (see in the text), it is not appropriate to exactly determine the aging effects on dynamical heterogeneities through the non-Gaussian parameter (e.g., through the mean-squared and the mean-quartic atomic displacements).

[30] Available at http://digitalfire.com/oxide/sio2.htm

[31] J. Horbach and W. Kob, Phys. Rev. B **60**, 3169 (1999).